

Supporting Information

The Influence of Glycans-Specific Bioconjugation on the FcγRI Binding and In Vivo Performance of ⁸⁹Zr-DFO-Pertuzumab

Delphine Vivier^{1,†}, Kimberly Fung^{1,2,†}, Cindy Rodriguez^{1,2}, Pierre Adumeau¹, Gary A. Ulaner^{3,4}, Jason S. Lewis^{3,4,5}, Sai Kiran Sharma^{3}, Brian M. Zeglis^{1,2,3*}*

¹ Department of Chemistry, Hunter College, City University of New York, New York, NY, USA

² Ph.D. Program in Chemistry, The Graduate Center of the City University of New York, New York, NY, USA

³Department of Radiology, Memorial Sloan Kettering Cancer Center, New York, NY, USA

⁴Department of Radiology, Weill Cornell Medical College, Center, New York, NY, USA

⁵Program in Molecular Pharmacology, Memorial Sloan Kettering Cancer Center, New York, NY, USA

[†]These two authors contributed equally to this work.

Co-Corresponding Authors:

Brian M. Zeglis: 413 East 69th Street, New York, NY, 10021. Phone: 212-896-0433. E-mail: bz102@hunter.cuny.edu

Sai Kiran Sharma: 1285 York Avenue, New York, NY, 10025. Phone: 212-896-0484. E-mail: sharmas@mskcc.org

TABLE OF CONTENTS

Supplemental Materials and Methods..... 3

 SDS-PAGE Analysis 3

 Size Exclusion Chromatography..... 3

 Flow Cytometry 3

 FcγRI Binding ELISA..... 4

 Radiolabeling with ⁸⁹Zr..... 4

 Bead-Based Immunoreactivity Assay..... 5

 Radioimmunoconjugate Stability Assays 5

 PET Imaging 6

 Acute Biodistribution Experiments..... 6

Supplemental Figures and Figure Captions 7

Supplemental Tables and Table Legends 16

SUPPLEMENTAL MATERIALS AND METHODS

SDS-PAGE Analysis

The purified constructs – pertuzumab, DFO-^{nss}pertuzumab, DFO-^{ss}pertuzumab-βGal, and DFO-^{ss}pertuzumab-EndoS – were characterized via sodium dodecyl sulfate-polyacrylamide gel electrophoresis (SDS-PAGE). Briefly, 2 μg antibody (0.85 μL of a 5.89 mg/mL stock) were combined with 31.65 μL H₂O, 5 μL 500 mM dithiothreitol (NuPAGE® 10X Sample Reducing Agent, Life Technologies), and 12.5 μL 4X electrophoresis buffer (NuPAGE® LDS Sample Buffer, Thermo Fisher, Eugene, OR). This mixture was then denatured by heating to 95°C for 10 min using a heat block. Subsequently, 20 μL of each sample was then loaded alongside an appropriate molecular weight marker (Mark12™ stained standard, Life Technologies) onto a 1 mm, 10 well 4-12% Bis-Tris protein gel (Life Technologies) and run for ~4 h at 10 V/cm in MOPS buffer. The completed gel was washed 3 times with H₂O, stained using SimplyBlue™ SafeStain (Life Technologies) for 1 h, and destained overnight in H₂O. The gel was then analyzed using an Odyssey Infrared Gel Scanner (Li-Cor Biosciences, Lincoln, NE).

Size Exclusion Chromatography

Size exclusion chromatography was performed on a Shimadzu UFLC HPLC system. 100 μg (0.67 nmol) of each construct was run on an SEC column (Superdex™ 200 Increase 10/300 GL, GE Healthcare) in phosphate buffered saline for 40 min (flow rate: 0.75 mL/min) and the absorbance was measured at 280 nm.

Flow Cytometry

Flow cytometry experiments were performed with HER2-positive BT474 cells. Native pertuzumab and the immunoconjugates were incubated at 6 μg/mL in suspension with 10⁶ cells/mL for 30 min on ice. Cells were washed three times by pelleting and resuspension and then incubated with a goat anti-human IgG-AlexaFluor568 secondary antibody (Thermo Fisher Scientific) at 4 μg/mL. Subsequently, the cells were again washed by pelleting and resuspension three times and then analyzed on a BD LSR II (BD Biosciences, San Jose, CA). Binding data was collected in triplicate, averaged, and plotted.

FcγRI Binding ELISA

Recombinant human Fc gamma RI/CD64, CF (R&D Systems # 1257-FC-050) was diluted to 10 µg/mL in sterile PBS and 100 µL/well was coated overnight at 4°C onto an ELISA plate (Nunc MaxiSorp® flat-bottom 96 well plate, Fisher Scientific). After a brief blocking period (40 min with PBS containing 10% FCS), the immunoconjugates were diluted in a blocking buffer (0.5 or 50 µg/mL) and 100 µL/well were applied for 2 h at room temperature. As not to disrupt the Fc-FcγRI interactions, the bound immunoconjugates were detected using 1: 5000 HRP-labeled anti human IgG (JacksonImmunoResearch Laboratories, West Grove, PA). After a final wash step, TMB substrate was used to develop the bound HRP secondary antibody, and the color reaction was stopped with 2N H₂SO₄. Optical Densities at 450 nm were determined using a SpectraMax i3 plate reader (Molecular Devices, San Jose, CA). Binding data was collected in triplicate, averaged, and plotted.

Radiolabeling with ⁸⁹Zr

For each antibody construct, 400 µg (2.67 nmol) of immunoconjugate solution was diluted in 400 µL PBS, pH 7.4. [⁸⁹Zr]Zr-oxalate (1300 µCi, 48.1 MBq) in 100 µL of 1.0 M oxalic acid was adjusted to pH 7.0-7.5 with 1.0 M Na₂CO₃. After the bubbling of CO₂ stopped, the ⁸⁹Zr solution was added to the antibody solution, and the resulting mixture was incubated at room temperature for 1 h. The reaction progress was then assayed using iTLC using an eluent of 50 mM EDTA (pH 5). Subsequently, the reaction was quenched with 10 µL of 50mM of EDTA (pH = 5), and the antibody construct was purified using size exclusion chromatography (Sephadex G-25 M, PD-10 column, GE Healthcare; dead volume = 2.5 mL, eluted with 500 µL fractions of PBS, pH 7.4). If necessary, the antibody was concentrated via centrifugal filtration units with a 50,000 Da molecular weight cut off (Amicon™ Ultra 4 Centrifugal Filtration Units, Millipore Corp. Billerica, MA). The radiochemical purity of the final radiolabeled bioconjugate was assayed by iTLC using 50 mM EDTA (pH 5) as an eluent. In the iTLC experiments, free [⁸⁹Zr]Zr⁴⁺ cations and [⁸⁹Zr]-EDTA elute with the solvent front, while the radioimmunoconjugate remains at the baseline.

Bead-Based Immunoreactivity Assay

A bead-based assay was used to determine the immunoreactive fraction of each of the immunoconjugates. To this end, 20 μL of Ni-NTA beads (Thermo Fisher Scientific # 88831) were transferred to EppendorfTM LoBind microcentrifuge tubes, and 380 μL of PBS-T (PBS with 0.05% Tween-20) was added. The tubes were vortexed for 5 sec, spun down, and placed on a DynaMag-2 magnetic rack (Invitrogen) for 30-45 sec. Once the beads settled, the supernatant was aspirated and discarded. The tubes were then placed on the magnetic rack, and 400 μL of PBS-T was added. 3 of the tubes were capped, labeled C₁-C₃, and set aside as controls.

Next, to prepare the antigen-coupled Ni-NTA beads, 1 μg (10 μL of 0.1 mg/mL dilution) of the His-tagged HER2 antigen (Acro Biosystems, Newark, DE) was added to the rest of the tubes (labeled T₁-T₃), and the tubes were placed on a rotating platform for 15 min. The tubes were then spun down and placed onto the magnetic rack, and the supernatant was aspirated. The same sequence of steps was repeated to wash the beads with 400 μL of PBS-T. Prior to addition of the radioimmunoconjugate in the next step, the beads were resuspended in 399 μL of 1% BSA-PBS.

Subsequently, each radioimmunoconjugates was diluted to 1 ng/ μL with PBS, and 1 ng of the diluted radioimmunoconjugate was added to all the tubes. The tubes were vortexed for 5 seconds and placed on the rotating platform for 30 min. The tubes were once again spun down and placed on the magnetic. The supernatant and two washes (400 μL each) were collected. Finally, the beads, supernatant, and washes were measured for radioactivity on a gamma counter (Automatic Wizard² γ -counter, Perkin Elmer, Inc., Waltham, MA). The immunoreactive fraction was then calculated as the fraction of activity associated with the beads corrected for the fraction of non-specific binding observed in the control samples.

Radioimmunoconjugate Stability Assays

The stability of the radioimmunoconjugates with respect to radiochemical purity and loss of radioactivity from the antibody was investigated via incubation of the antibodies in human serum for 7 days at 37°C (n = 3). At predetermined time intervals, the radiochemical purity of the radioimmunoconjugates was determined via iTLC with an eluent of 50 mM EDTA pH 5.0.

PET Imaging

PET imaging experiments were conducted on a microPET Focus rodent scanner (Concorde Microsystems). Mice (athymic nude or humanized NSG mice) bearing subcutaneous BT474 xenografts (left shoulder, 60-120 mm³, 25-30 days after inoculation) were administered the radioimmunoconjugates [175-210 µCi, 6.5-7.8 MBq (40-80 µg) in 200 µL of saline] via tail vein injection. Approximately 5 min before PET imaging, the mice were anesthetized by inhalation of a 2% isoflurane (Baxter Healthcare):oxygen gas mixture and placed on the scanner bed. Anesthesia was maintained using a 1% isoflurane mixture. PET data for each mouse were recorded via static scans at 24, 48, 96 and 144 h post-injection (n = 4-5 per group).

Acute Biodistribution Experiments

Mice (athymic nude or humanized NSG mice) bearing subcutaneous BT474 xenografts (left shoulder; 60-120 mm³) were randomized before the study and were administered the radioimmunoconjugates [20 µCi, 0.74 MBq (10 µg) in 200 µL of saline] via tail vein injection. Subsequently, the animals (n = 5 per group) were euthanized by CO₂(g) asphyxiation at 24, 48, 96, and 144 h p.i., and 13 tissues (including the tumor) were removed, washed, dried, weighed, and counted in a gamma counter (PerkinElmer, Inc.). The number of counts in each tissue were background and decay corrected to the time of injection and converted to activity units (µCi) using a calibration curve generated from known standards. The %ID/g for each tissue sample was then calculated by normalization to the total activity injected and the mass of each tissue.

SUPPLEMENTAL FIGURES AND FIGURE CAPTIONS

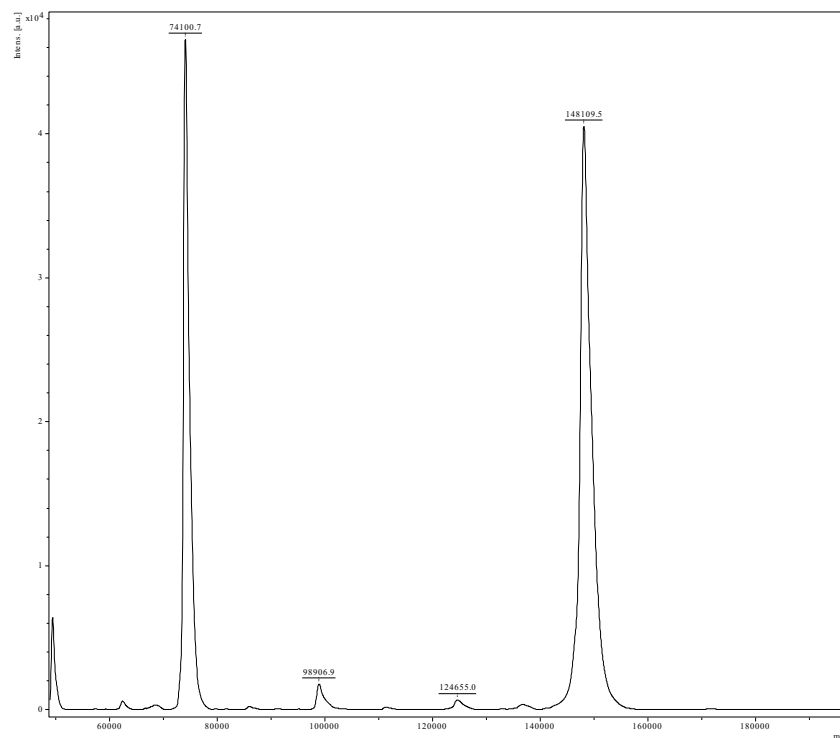


Figure S1. Representative MALDI-ToF spectrum for native pertuzumab.

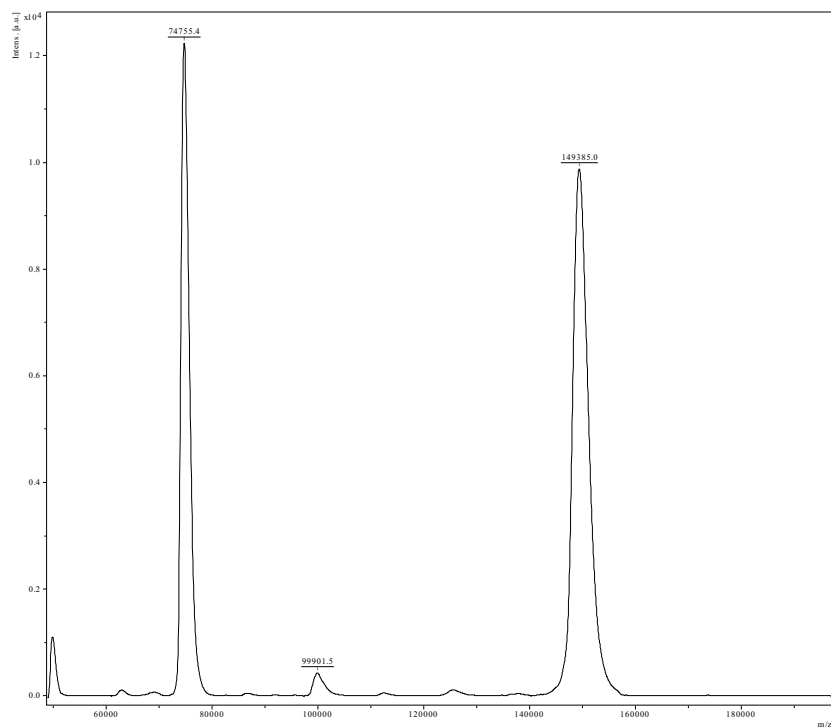


Figure S2. Representative MALDI-ToF spectrum for DFO-nss pertuzumab.

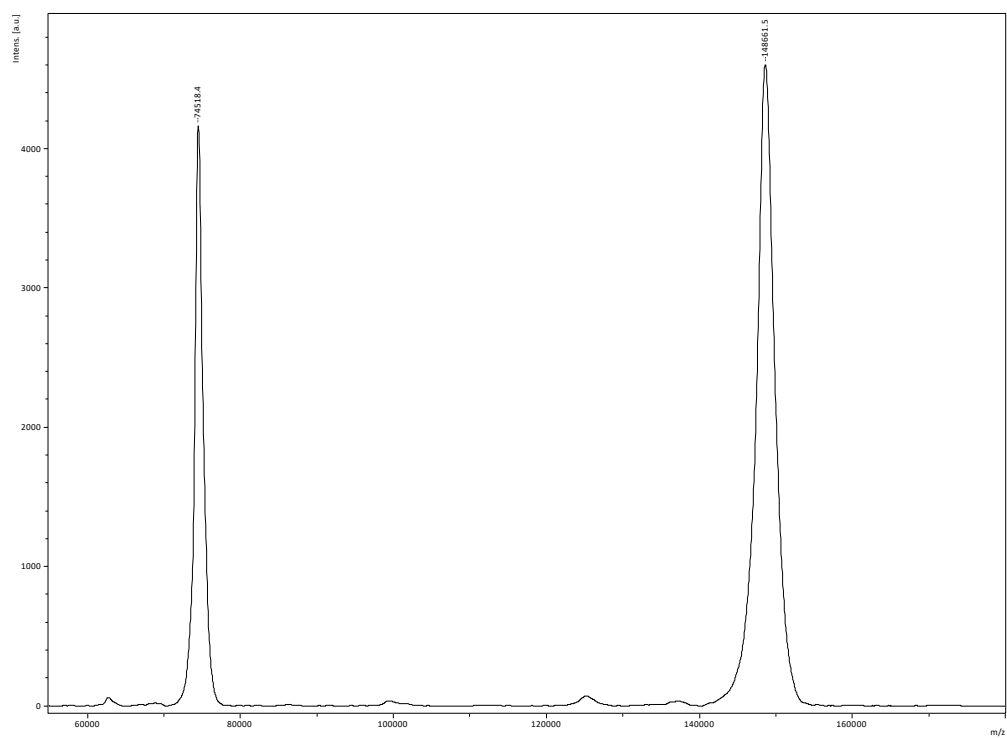


Figure S3. Representative MALDI-ToF spectrum for N₃-sspertuzumab-βGal.

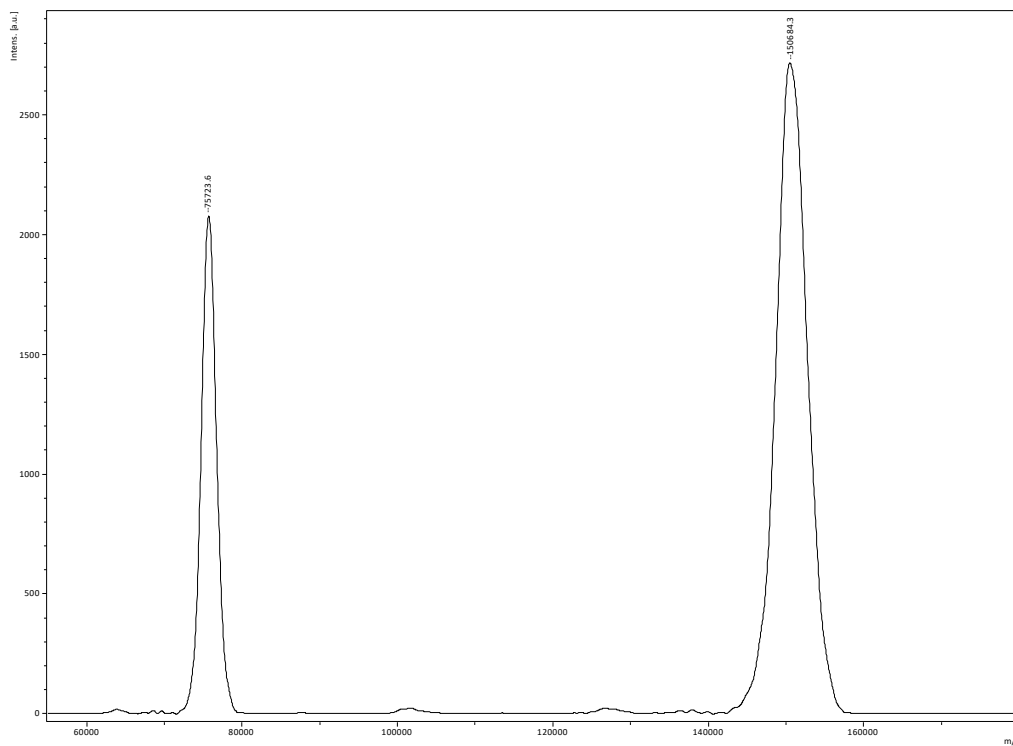


Figure S4. Representative MALDI-ToF spectrum for DFO-sspertuzumab-βGal.

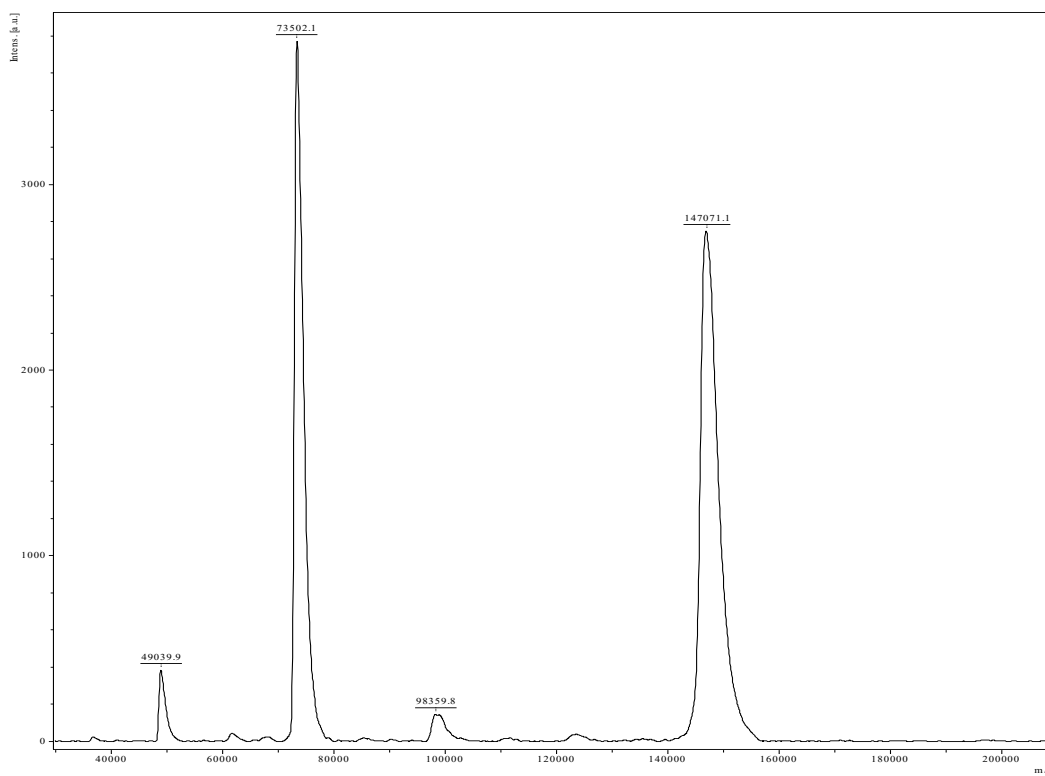


Figure S5. Representative MALDI-ToF spectrum for N₃-^{ss}pertuzumab-EndoS.

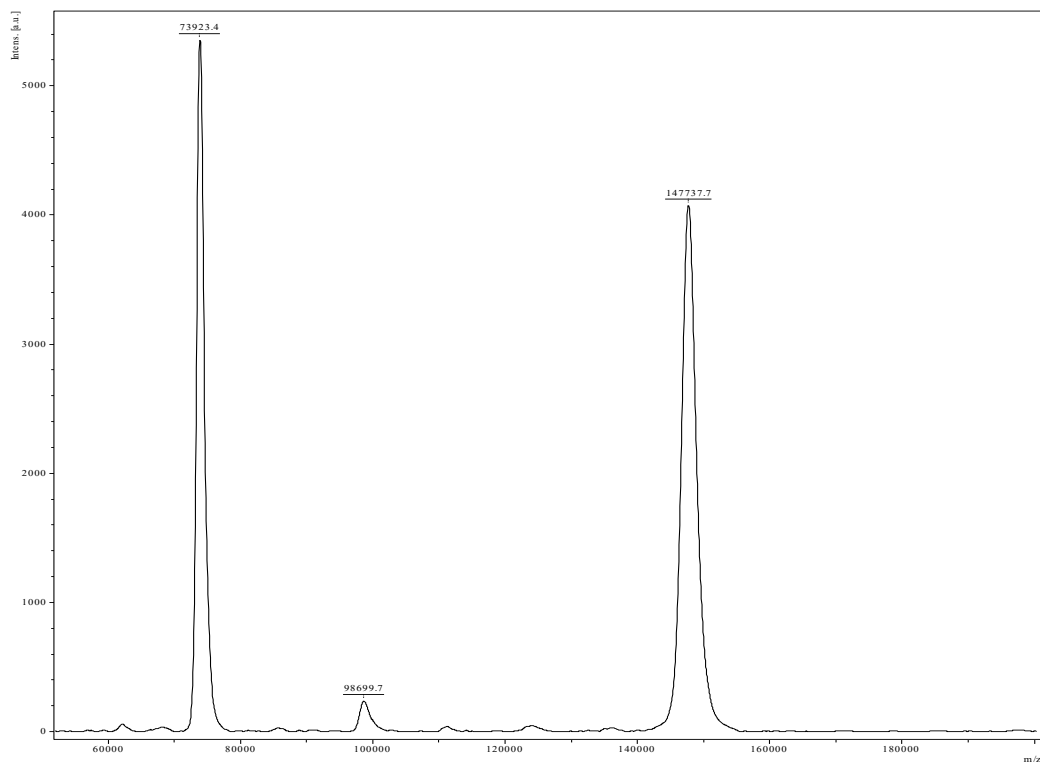


Figure S6. Representative MALDI-ToF spectrum for DFO-^{ss}pertuzumab-EndoS.

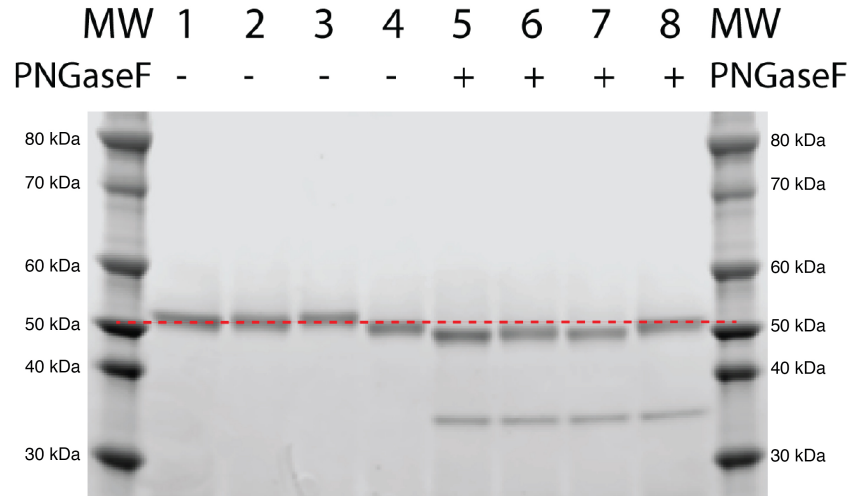


Figure S7. Denaturing SDS-PAGE of unmodified pertuzumab (1 & 5), DFO-^{nss}pertuzumab (2 & 6), DFO-^{ss}pertuzumab-βGal (3 & 7), and DFO-^{ss}pertuzumab-EndoS (4 & 8) before (1-4) and after (5-8) PNGaseF-mediated deglycosylation. After deglycosylation, the heavy chain of each of the immunoconjugates has the same molecular weight, except that DFO-^{ss}pertuzumab-EndoS (because PNGaseF is unable to digest the immunoconjugate's truncated glycans). The red dotted line denotes the mass of the heavy chain of native pertuzumab.

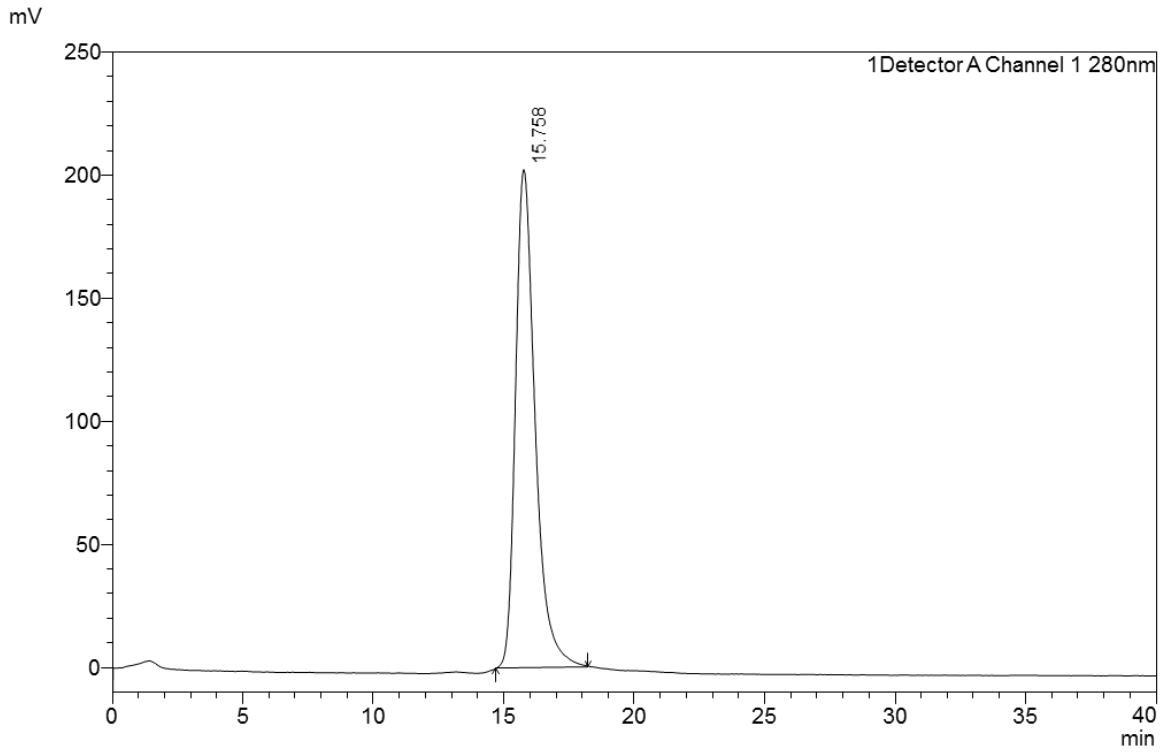


Figure S8. Size exclusion chromatogram of native pertuzumab

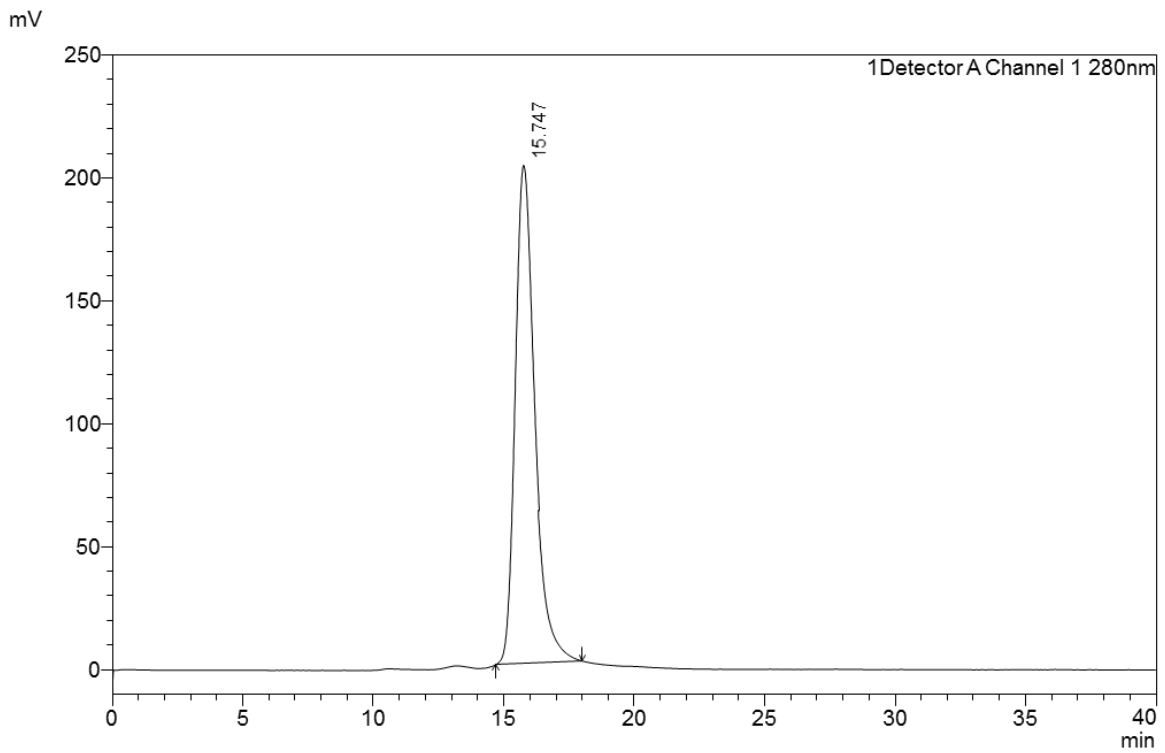


Figure S9. Size exclusion chromatogram of DFO-^{nss} pertuzumab.

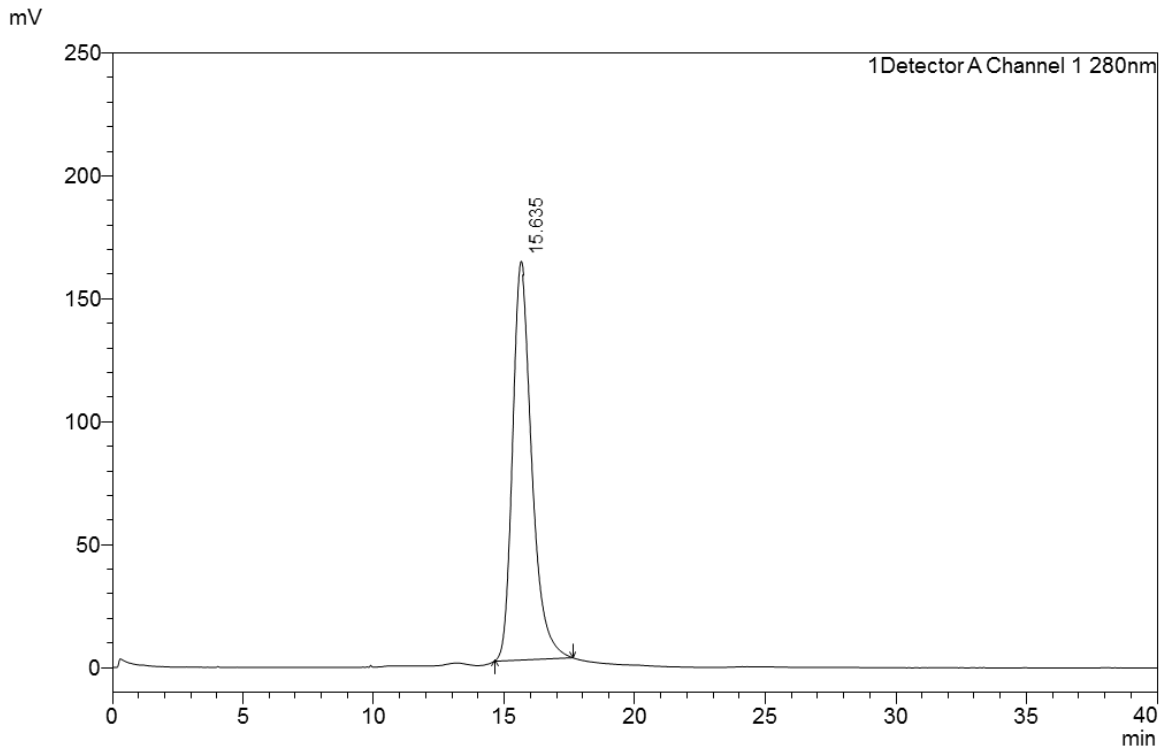


Figure S10. Size exclusion chromatogram of DFO-^{ss}pertuzumab- β Gal.

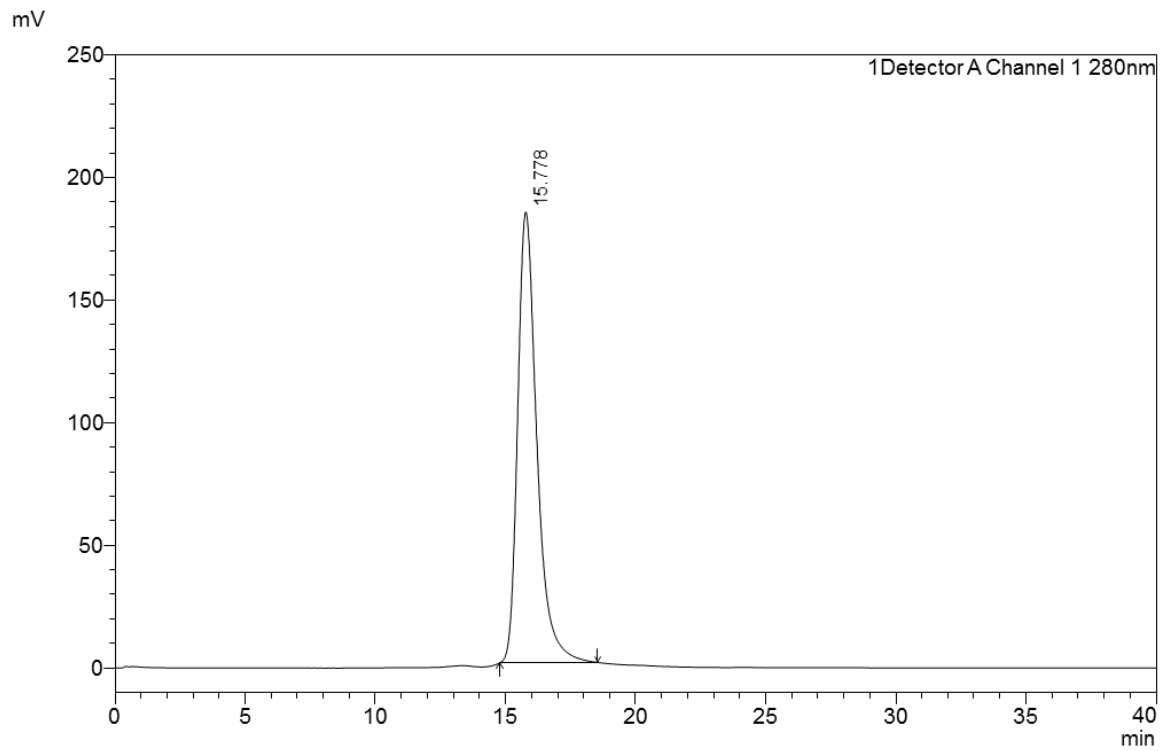


Figure S11. Size exclusion chromatogram of DFO-^{ss}pertuzumab-EndoS.

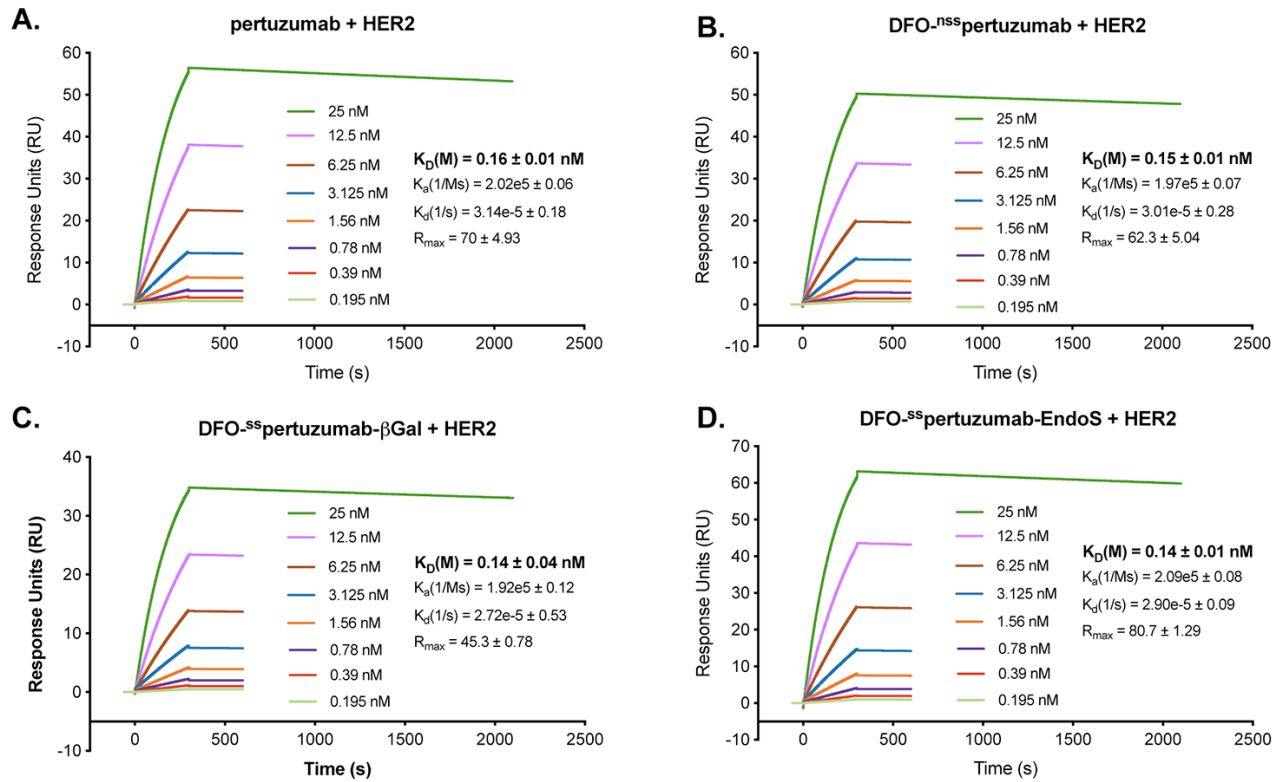


Figure S12. SPR sensorgrams for the binding of (A) native pertuzumab, (B) DFO^{nss}pertuzumab, (C) DFO^{ss}pertuzumab-EndoS, and (D) DFO^{ss}pertuzumab-βGal to recombinant HER2.

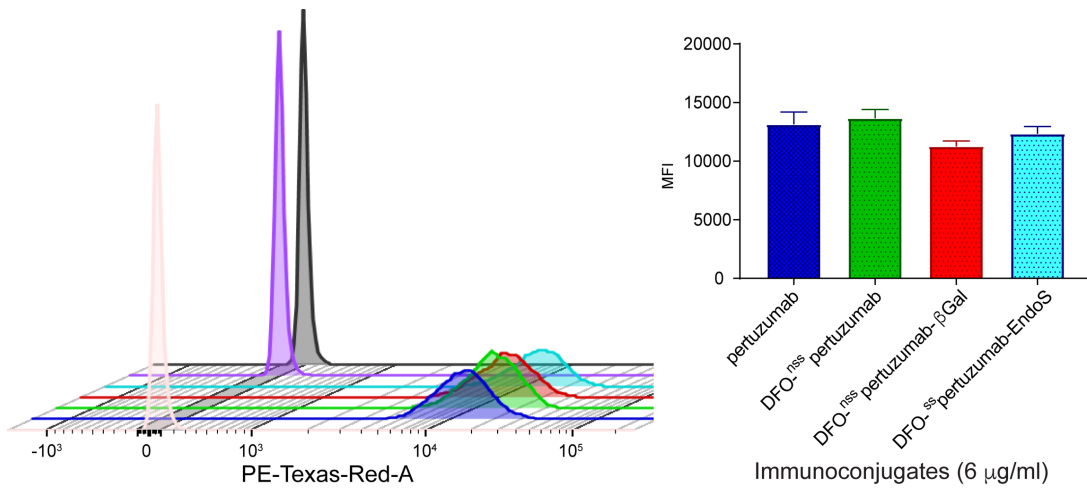


Figure S13. Flow cytometry data showing the binding of the immunoconjugates to HER2-expressing BT474 human breast cancer cells.

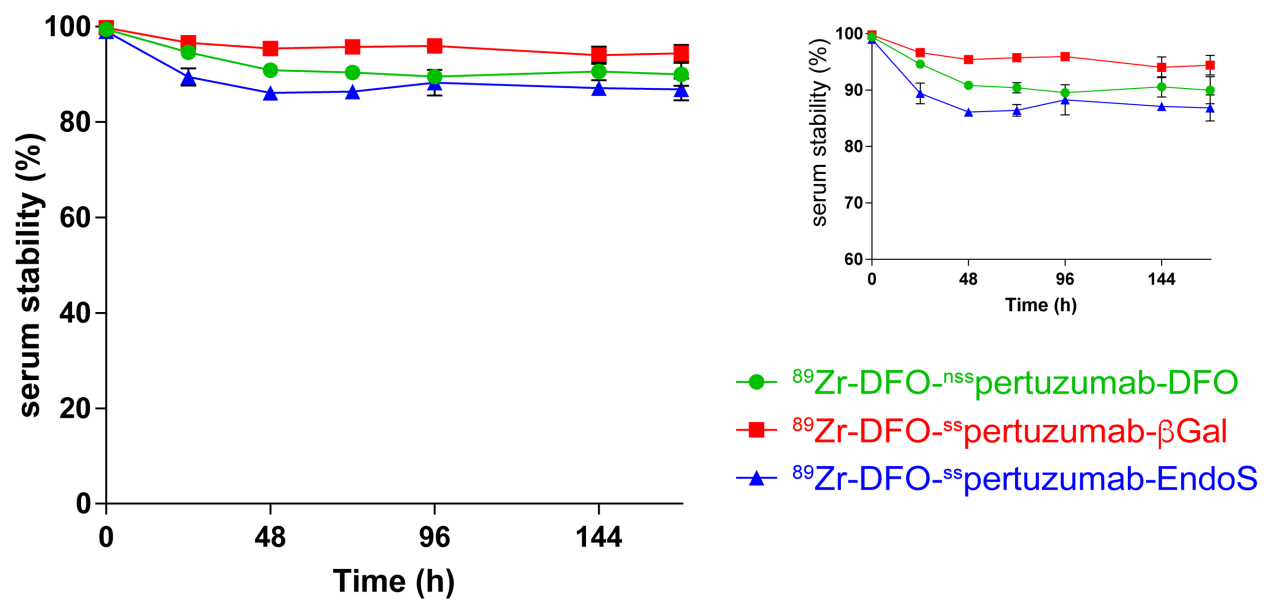


Figure S14. Stability of the three radioimmunoconjugates to demetallation in human serum at 37°C. Measurements were collected using radio-iTLC and performed in triplicate.

SUPPLEMENTAL TABLES AND TABLE LEGENDS

Constructs	Average mass (Da)	Degree of Labeling (DFO/mAb)
pertuzumab	148264 ± 110	1.4 ± 0.4
DFO- ^{nss} pertuzumab	149300 ± 185	
N ₃ - ^{ss} pertuzumab-βGal	148645 ± 12	2.6 ± 0.1
DFO- ^{ss} pertuzumab-βGal	150574 ± 86	
N ₃ - ^{ss} pertuzumab-EndoS	147145 ± 59	1.3 ± 0.2
DFO- ^{ss} pertuzumab-EndoS	146998 ± 60	

Table S1. Degree of labeling of each immunoconjugate as determined via MALDI-MS.

	⁸⁹ Zr-DFO- ^{nss} pertuzumab				⁸⁹ Zr-DFO- ^{ss} pertuzumab-βGal				⁸⁹ Zr-DFO- ^{ss} pertuzumab-EndoS			
	24 h	48 h	96 h	144 h	24 h	48 h	96 h	144 h	24 h	48 h	96 h	144 h
Blood	9.22 ± 0.72	7.17 ± 2.68	5.42 ± 2.16	4.88 ± 2.09	10.41 ± 0.95	8.18 ± 3.29	7.86 ± 1.36	5.77 ± 1.53	9.84 ± 0.84	8.33 ± 3.31	6.12 ± 2.11	4.70 ± 2.12
Tumor	30.99 ± 1.84	45.36 ± 10.54	41.30 ± 10.54	93.15 ± 52.16	31.60 ± 2.10	47.88 ± 14.39	61.05 ± 10.67	77.15 ± 32.99	35.60 ± 9.12	54.64 ± 18.38	64.43 ± 23.38	76.68 ± 28.67
Heart	3.11 ± 0.85	2.84 ± 1.11	1.89 ± 0.71	1.90 ± 0.80	3.88 ± 0.75	2.77 ± 1.18	2.75 ± 0.94	1.86 ± 0.30	3.39 ± 0.47	3.02 ± 1.30	2.12 ± 0.77	1.78 ± 0.79
Lung	4.40 ± 0.65	3.65 ± 1.04	3.06 ± 1.01	2.90 ± 0.98	4.09 ± 0.55	3.79 ± 1.53	4.36 ± 0.88	3.72 ± 0.97	4.13 ± 0.65	4.14 ± 1.61	3.55 ± 1.10	2.84 ± 1.21
Liver	3.37 ± 0.50	3.86 ± 1.76	4.10 ± 1.19	4.50 ± 2.38	2.51 ± 0.33	3.56 ± 1.26	4.92 ± 2.21	5.22 ± 2.04	1.96 ± 0.08	2.43 ± 0.65	2.47 ± 1.02	2.47 ± 1.17
Spleen	2.04 ± 0.34	2.41 ± 1.05	1.96 ± 0.97	1.68 ± 0.53	1.71 ± 0.21	2.11 ± 0.65	1.94 ± 0.59	1.99 ± 0.43	1.87 ± 0.14	1.91 ± 0.62	1.75 ± 0.34	1.77 ± 0.53
Stomach	1.35 ± 0.71	0.77 ± 0.22	0.63 ± 0.22	0.45 ± 0.18	0.79 ± 0.35	0.78 ± 0.44	0.62 ± 0.16	0.53 ± 0.15	0.70 ± 0.27	0.90 ± 0.31	0.67 ± 0.38	0.54 ± 0.27
SI	1.21 ± 0.19	1.22 ± 0.51	0.88 ± 0.42	0.63 ± 0.27	1.11 ± 0.20	0.98 ± 0.36	1.03 ± 0.19	0.63 ± 0.05	1.13 ± 0.11	1.03 ± 0.35	0.78 ± 0.24	0.63 ± 0.32
LI	1.47 ± 0.31	1.40 ± 0.39	0.96 ± 0.43	0.69 ± 0.15	1.02 ± 0.47	0.90 ± 0.20	0.82 ± 0.07	0.66 ± 0.16	0.99 ± 0.71	0.73 ± 0.22	0.92 ± 0.22	0.48 ± 0.15
Kidney	3.74 ± 0.12	3.52 ± 0.64	3.56 ± 0.59	3.47 ± 0.85	3.81 ± 0.35	4.10 ± 0.90	5.40 ± 0.54	5.72 ± 1.21	3.63 ± 0.41	4.49 ± 1.16	4.25 ± 1.24	4.86 ± 1.57
Muscle	0.81 ± 0.41	0.90 ± 0.32	0.60 ± 0.14	0.60 ± 0.21	1.08 ± 0.11	0.76 ± 0.21	0.84 ± 0.29	0.71 ± 0.34	1.08 ± 0.31	0.91 ± 0.23	0.51 ± 0.14	0.49 ± 0.16
Bone	1.87 ± 0.48	3.94 ± 3.32	5.25 ± 3.39	8.42 ± 2.36	1.28 ± 0.41	1.78 ± 0.50	2.24 ± 0.44	2.68 ± 0.66	1.81 ± 0.60	3.00 ± 0.69	4.06 ± 1.32	6.50 ± 0.96
Skin	3.73 ± 0.37	4.44 ± 0.55	3.15 ± 1.07	2.55 ± 0.94	4.64 ± 0.59	4.51 ± 1.97	4.78 ± 1.58	5.38 ± 2.56	3.77 ± 0.66	5.06 ± 2.37	3.59 ± 2.50	4.09 ± 3.00

Table S2. Biodistribution data for the three constructs in nude mice bearing BT474 subcutaneous xenografts. The values are %ID/g ± SD; n = 5 mice for each time point and radioimmunoconjugate. SI = small intestine; LI = large intestine. The stomach, SI, and LI values include contents.

Tumor/	⁸⁹ Zr-DFO- ^{nss} pertuzumab				⁸⁹ Zr-DFO- ^{ss} pertuzumab-βGal				⁸⁹ Zr-DFO- ^{ss} pertuzumab-EndoS			
	24 h	48 h	96 h	144 h	24 h	48 h	96 h	144 h	24 h	48 h	96 h	144 h
Blood	3.36 ± 0.33	6.32 ± 2.78	7.62 ± 3.61	19.10 ± 13.47	3.04 ± 0.34	5.86 ± 2.94	7.76 ± 1.91	13.37 ± 6.73	3.62 ± 0.98	6.56 ± 3.42	10.52 ± 5.27	16.31 ± 9.55
Heart	9.97 ± 2.79	15.95 ± 7.24	21.84 ± 9.95	49.05 ± 34.41	8.14 ± 1.67	17.30 ± 9.02	22.19 ± 8.50	41.58 ± 19.02	10.51 ± 3.06	18.10 ± 9.88	30.43 ± 15.62	43.06 ± 24.95
Lung	7.05 ± 1.12	12.44 ± 4.56	13.50 ± 5.65	32.14 ± 21.04	7.73 ± 1.16	12.65 ± 6.38	14.01 ± 3.75	20.73 ± 10.39	8.62 ± 2.59	13.20 ± 6.80	18.17 ± 8.69	27.04 ± 16.66
Liver	9.19 ± 1.48	11.75 ± 6.02	10.07 ± 3.89	20.68 ± 15.94	12.60 ± 1.85	13.46 ± 6.26	12.40 ± 5.98	14.79 ± 8.58	18.20 ± 4.73	22.51 ± 9.66	26.05 ± 14.27	31.02 ± 19.78
Spleen	15.17 ± 2.67	18.79 ± 9.28	21.05 ± 11.71	55.54 ± 35.63	18.47 ± 2.59	22.66 ± 9.77	31.53 ± 11.12	38.71 ± 18.51	19.08 ± 5.08	28.55 ± 13.29	36.71 ± 15.14	43.33 ± 24.22
Stomach	22.98 ± 12.14	58.67 ± 21.81	66.01 ± 28.60	206.49 ± 142.31	40.16 ± 17.87	61.42 ± 39.57	98.09 ± 30.03	146.09 ± 75.09	51.06 ± 23.73	60.40 ± 29.09	95.78 ± 64.52	143.29 ± 84.49
SI	25.69 ± 4.26	37.31 ± 17.98	46.97 ± 25.34	147.32 ± 103.77	28.43 ± 5.54	48.68 ± 22.90	59.25 ± 14.88	121.94 ± 53.13	31.63 ± 8.66	52.87 ± 25.39	82.89 ± 39.71	120.89 ± 86.03
LI	21.15 ± 4.66	32.33 ± 11.70	42.93 ± 22.25	135.04 ± 81.33	31.09 ± 14.45	52.97 ± 19.72	74.19 ± 14.36	117.47 ± 58.16	35.97 ± 27.37	74.96 ± 34.16	70.36 ± 30.47	161.07 ± 94.37
Kidney	8.28 ± 0.56	12.90 ± 3.80	11.59 ± 3.53	26.84 ± 16.41	8.30 ± 0.95	11.67 ± 4.34	11.30 ± 2.27	13.49 ± 6.44	9.79 ± 2.74	12.16 ± 5.15	15.15 ± 7.06	15.78 ± 7.06
Muscle	38.25 ± 19.36	50.43 ± 21.37	69.04 ± 24.18	156.35 ± 104.07	29.13 ± 3.64	63.04 ± 25.70	72.85 ± 28.14	109.22 ± 70.84	32.99 ± 12.79	59.73 ± 24.99	126.32 ± 57.76	157.71 ± 71.93
Bone	16.55 ± 4.32	11.51 ± 10.07	7.86 ± 5.46	11.06 ± 6.93	24.72 ± 8.06	26.93 ± 11.11	27.31 ± 7.23	28.75 ± 14.17	19.71 ± 8.29	18.24 ± 7.42	15.86 ± 7.71	11.81 ± 4.18
Skin	8.31 ± 0.95	10.22 ± 2.70	13.11 ± 5.58	36.52 ± 24.46	6.81 ± 0.97	10.61 ± 5.62	12.78 ± 4.78	14.34 ± 9.18	9.44 ± 2.93	10.79 ± 6.23	17.97 ± 14.14	18.75 ± 14.03

Table S3. Tumor-to-tissue activity concentration ratios for the three constructs in nude mice bearing BT474 subcutaneous xenografts. The values are %ID/g ± SD; n = 5 mice for each time point and radioimmunoconjugate. SI = small intestine; LI = large intestine. The stomach, SI, and LI values include contents.

	⁸⁹ Zr-DFO- ^{nss} pertuzumab	⁸⁹ Zr-DFO- ^{ss} pertuzumab-βGal	⁸⁹ Zr-DFO- ^{ss} pertuzumab-EndoS
	<i>144 h</i>	<i>144 h</i>	<i>144 h</i>
Blood	1.03 ± 0.63	4.51 ± 3.00	8.76 ± 2.31
Tumor	46.13 ± 16.46	77.53 ± 12.56	111.84 ± 39.88
Heart	0.90 ± 0.04	1.76 ± 0.78	2.56 ± 0.23
Lung	2.40 ± 0.50	4.41 ± 1.49	6.55 ± 1.07
Liver	10.25 ± 2.74	8.87 ± 3.53	4.71 ± 0.77
Spleen	44.77 ± 7.92	22.39 ± 17.37	13.09 ± 3.99
Stomach	0.74 ± 0.22	1.08 ± 0.78	0.88 ± 0.25
SI	2.69 ± 0.53	2.44 ± 0.62	1.99 ± 0.49
LI	1.00 ± 0.07	0.92 ± 0.44	1.20 ± 0.73
Kidney	3.94 ± 1.97	5.44 ± 0.65	4.43 ± 0.72
Muscle	0.63 ± 0.17	0.69 ± 0.11	0.90 ± 0.18
Bone	9.14 ± 3.05	5.84 ± 2.11	7.24 ± 2.04
Skin	2.44 ± 0.29	5.34 ± 3.57	4.64 ± 2.20

Table S4. Biodistribution data for the three radioimmunoconjugates at 144 h post-injection in humanized NSG mice bearing BT474 subcutaneous xenografts. The values are %ID/g ± SD; n = 4 mice for ⁸⁹Zr-DFO-^{nss}pertuzumab, n = 5 mice for ⁸⁹Zr-DFO-^{ss}pertuzumab-βGal, and n = 5 mice for ⁸⁹Zr-DFO-^{ss}pertuzumab-EndoS. SI = small intestine; LI = large intestine. The stomach, SI, and LI values include contents.

	⁸⁹ Zr-DFO- ^{nss} pertuzumab	⁸⁹ Zr-DFO- ^{ss} pertuzumab-βGal	⁸⁹ Zr-DFO- ^{ss} pertuzumab-EndoS
<i>Tumor/</i>	<i>144 h</i>	<i>144 h</i>	<i>144 h</i>
Blood	44.91 ± 19.91	17.21 ± 11.78	12.77 ± 5.66
Heart	51.30 ± 18.42	43.95 ± 20.71	43.73 ± 16.08
Lung	19.21 ± 7.93	17.57 ± 6.58	17.09 ± 6.70
Liver	4.50 ± 2.01	8.74 ± 3.75	23.72 ± 9.30
Spleen	1.03 ± 0.41	3.46 ± 2.75	8.54 ± 4.01
Stomach	62.14 ± 28.82	71.89 ± 53.04	127.34 ± 57.69
SI	17.13 ± 6.98	31.84 ± 9.60	56.26 ± 24.41
LI	46.08 ± 16.79	84.15 ± 42.52	93.44 ± 65.84
Kidney	11.72 ± 7.20	14.26 ± 2.87	25.23 ± 9.90
Muscle	73.33 ± 32.53	112.22 ± 25.95	124.41 ± 50.67
Bone	5.05 ± 2.47	13.28 ± 5.27	15.45 ± 7.02
Skin	18.90 ± 7.11	14.53 ± 10.01	24.12 ± 14.33

Table S5. Tumor-to-tissue activity concentration ratios for the three radioimmunoconjugates at 144 h post-injection in humanized NSG mice bearing BT474 subcutaneous xenografts. The values are %ID/g ± SD; n = 4 mice for ⁸⁹Zr-DFO-^{nss}pertuzumab, n = 5 mice for ⁸⁹Zr-DFO-^{ss}pertuzumab-βGal, and n = 5 mice for ⁸⁹Zr-DFO-^{ss}pertuzumab-EndoS. SI = small intestine; LI = large intestine. The stomach, SI, and LI values include contents.